Discrete Mathematics and Theoretical Computer Science DMTCS vol. **17:1**, 2015, 219–240

A Conjecture on the Number of Hamiltonian Cycles on Thin Grid Cylinder Graphs

Olga Bodroža-Pantić[1*] Harris Kwong[2†] Milan Pantić[3‡]

[1]*Dept. of Math. & Info., Faculty of Science, University of Novi Sad, Serbia*
[2]*Dept. of Math. Sci., SUNY at Fredonia, NY, U.S.A.*
[3]*Dept. of Physics, Faculty of Science, University of Novi Sad, Serbia*

received 16th Mar. 2014, revised 27th Jan. 2015, 25th Mar. 2015, accepted 25th Mar. 2015.

We study the enumeration of Hamiltonian cycles on the thin grid cylinder graph $C_m \times P_{n+1}$. We distinguish two types of Hamiltonian cycles depending on their contractibility (as Jordan curves) and denote their numbers $h_m^{nc}(n)$ and $h_m^c(n)$. For fixed m, both of them satisfy linear homogeneous recurrence relations with constant coefficients. We derive their generating functions and other related results for $m \leq 10$. The computational data we gathered suggests that $h_m^{nc}(n) \sim h_m^c(n)$ when m is even.

Keywords: Hamiltonian cycles, generating functions, thin grid cylinder, contractible curves.

1 Introduction

A Hamiltonian path of a simple graph is a path that visits each vertex exactly once. A closed Hamiltonian path is called a Hamiltonian cycle or Hamiltonian circuit, which we shall abbreviate as HC. The enumeration of Hamiltonian cycles on rectangular grid graphs $P_m \times P_n$ had been studied extensively in, among others, [2, 4, 9, 15, 10, 13, 14, 17, 19, 20]. In contrast, little work [2, 9, 11, 17] was devoted to enumerate Hamiltonian cycles on rectangular grid cylinders $C_m \times P_n$.

In this paper we investigate, for each fixed $m \geq 2$, the generation and enumeration of Hamiltonian cycles on $C_m \times P_{n+1}$, where $n \geq 1$. Since n grows while m is fixed, such graphs are called ***thin grid cylinders*** in the literature. In [2], vertices were encoded. We adopt a different approach by coding the cells or squares on the cylindrical surface, along with the so-called k-SIST equivalence relation. This equivalence relation was formerly called k-SISET, and was first used in [4] to enumerate Hamiltonian cycles on $P_m \times P_n$. A very similar approach for the same enumeration was implemented in [19] using the language of finite automa.

*Email: `bodroza@dmi.uns.ac.rs`. Research supported by the Ministry of Education and Science of the Republic of Serbia (Grants OI 174018, and III 46005).

†Email: `kwong@fredonia.edu`.

‡Email: `mpantic@df.uns.ac.rs`. Research supported by the Ministry of Education and Science of the Republic of Serbia (Grants OI 171009).

We distinguish two different types of HCs. In the sense of homotopy: one type of HCs are contractible (as Jordan curves) to a point, and the other type of HCs are not. We denote them HC^c and HC^{nc}, respectively. Simply put, a HC^{nc} is one that "perches" on or wraps around the cylinder likes a bracelet on an arm, and a HC^c can be "pasted" on the cylindrical surface. Let $h_m^{nc}(n)$ and $h_m^c(n)$ be the number of HC^{nc}s and HC^{c}s, respectively, on $C_m \times P_{n+1}$, Our objective is to determine, for each fixed m, the sequences $h_n^{nc} = \{h_m^{nc}(n)\}_{n\geq 1}$ and $h_m^c = \{h_m^c(n)\}_{n\geq 1}$. It is obvious that the number of HCs on $C_m \times P_{n+1}$ is given by $h_m(n) = h_m^{nc}(n) + h_m^c(n)$.

We characterize both types of HCs, and use it to define, for each fixed $m \geq 2$, a digraph $\mathcal{D}_m$. The original enumeration problem is equivalent to counting oriented walks of length $n-1$ in this digraph with first and last vertices from two special sets. Using the transfer matrix method [5, 18], we obtain the generating functions for the sequences h_m^{nc} and h_m^c, thereby proving that they both satisfy some linear homogeneous recurrence relations with constant coefficients.

For each fixed m, these two generating functions share the same denominator, hence the same recurrence relation. We used Pascal programs and Mathematica 6 to carry out the computation. Our results agree with those reported in [2, 11], which used a different approach. The computational data from $m = 2, 4, 6, 8, 10$ suggest that $h_m^{nc}(n)$ and $h_m^c(n)$ have the same number of digits and start with the same sequence of digits. For example,

$$
\begin{aligned}
h_{10}^{nc}(100) &= 1061896619979829012626416948662607870813534906540453497737 84\\
& 0084834119886910352471145024757227674029872331902823877569 09\\
& 370114350307029109724547376329803161998226608 2,\\
h_{10}^{c}(100) &= 1061896619971336297771539676279912074371931455713622590967 52\\
& 8050560079924636346860460526055405876433242946170400456707 14\\
& 114349734664774259331660887756923323923811144 0.
\end{aligned}
$$

Both numbers have 166 digits, and their first 12 digits are identical. Why is this happening?

2 Preliminaries

The graph $C_m \times P_{n+1}$ can be drawn on a cylindrical surface in such a way that no edges cross each other, see Figure 1. There are mn squares (4-cycles) called ***windows***. Label the vertices (i, j) and the windows $w_{i,j}$, where $1 \leq i \leq m$, $1 \leq j \leq n+1$ for vertices, and $1 \leq j \leq n$ for windows, as shown in Figure 1. Construct a ***window lattice graph*** $W_{m,n}$ with vertices representing the windows of $C_m \times P_{n+1}$, and two vertices are adjacent if and only if their corresponding windows in $C_m \times P_{n+1}$ share a common edge. It should be clear that $W_{m,n}$ is isomorphic to $C_m \times P_n$.

We distinguish two types of closed Jordan curves on a cylindrical surface: those that divide the surface into two infinite regions (image the cylinder being extended indefinitely in both directions to the left and to the right), see the curve $\mathcal{K}^{nc}$ in Figure 2, and those that divide the surface into one finite and one infinite region, see the curve $\mathcal{K}^c$ in Figure 2. The first type (non-contractible HC) wraps around the cylindrical surface, hence divides the cylindrical surface into the left half and the right half, it resembles a bracelet around an arm. The second type (contractible HC) encloses a finite region and leaves an infinite region on the outside. One could imagine it being pasted onto the cylindrical surface.

We abbreviate these two types of Hamiltonian cycles as HC^{nc} and HC^c, respectively. We use the following convention to name the two regions separated by a HC:

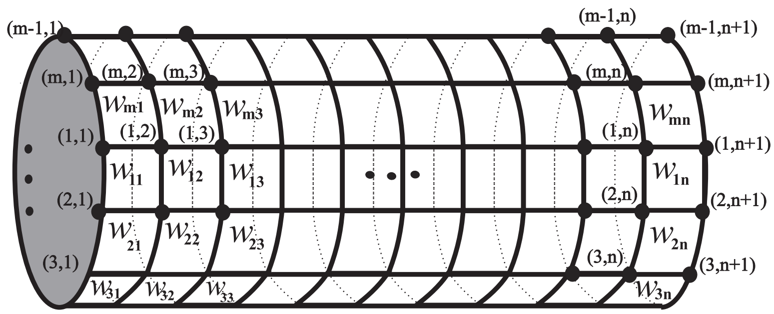

Fig. 1: The labeled graph $C_m \times P_{n+1}$ and its windows.

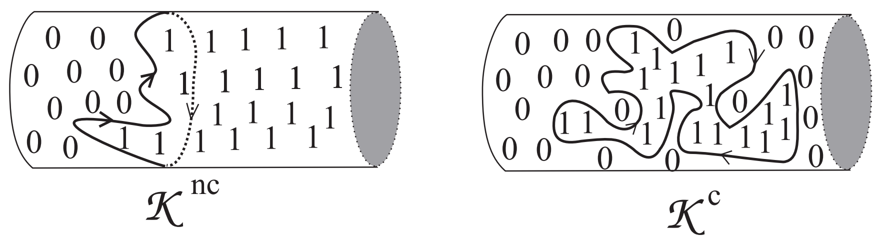

Fig. 2: Two types of closed Jordan curves on a cylindrical surface.

- For a non-contractible HC: all edges that connect two adjacent vertices from $\{(i, 1) \mid 1 \leq i \leq m\}$, but do not lie on the HC, belong to the same region. We call this region (on the left of the HC) the ***zero region***, and the other region (on the right of the HC) the ***positive region***.
- For a contractible HC: the windows within the bounded region are marked with 1s, hence the bounded region is the ***positive region***, which makes the exterior unbounded region the ***zero region***.

Alternatively, the orientation of the HC is chosen such that the zero region is always on our left as we traverse through the HC (see Figure 3). For HC^c this orientation is in the clockwise direction.

We use $h_m^{nc}(n)$ and $h_m^c(n)$ to indicate the number of HC^{nc}s and HC^{c}s. Their respective generating functions are written as $\mathcal{H}_m^{nc}(x)$ and $\mathcal{H}_m^c(x)$. Using a standard parity argument (likes the one used on a checkerboard), it is easy to tell which thin grid cylinders have a Hamiltonian cycle.

Theorem 2.1 *For $m \geq 2$ and $n \geq 1$, we have $h_m^{nc}(n) = 0$ if and only if both m and n are odd, and $h_m^c(n) = 0$ if and only if m is odd and n is even.*

Proof: It is straightforward to construct a HC^{nc} for even m or even n, and a HC^c for even m or odd n (see Figure 4). It remains to establish the condition under which no HC exists.

Consider the "vertical" edges joining vertices (m, i) to $(1, i)$ for $1 \leq i \leq n+1$, see Figure 3. Any HC may contain some of these vertical edges, and the number of such edges is odd for a HC^{nc}, and even for a HC^c.

As we travel along a non-contractible Hamiltonian cycle, the number of steps "to the left" and "to the right" must be equal, while the difference between the "up" and "down" steps is m. Since the HC contains

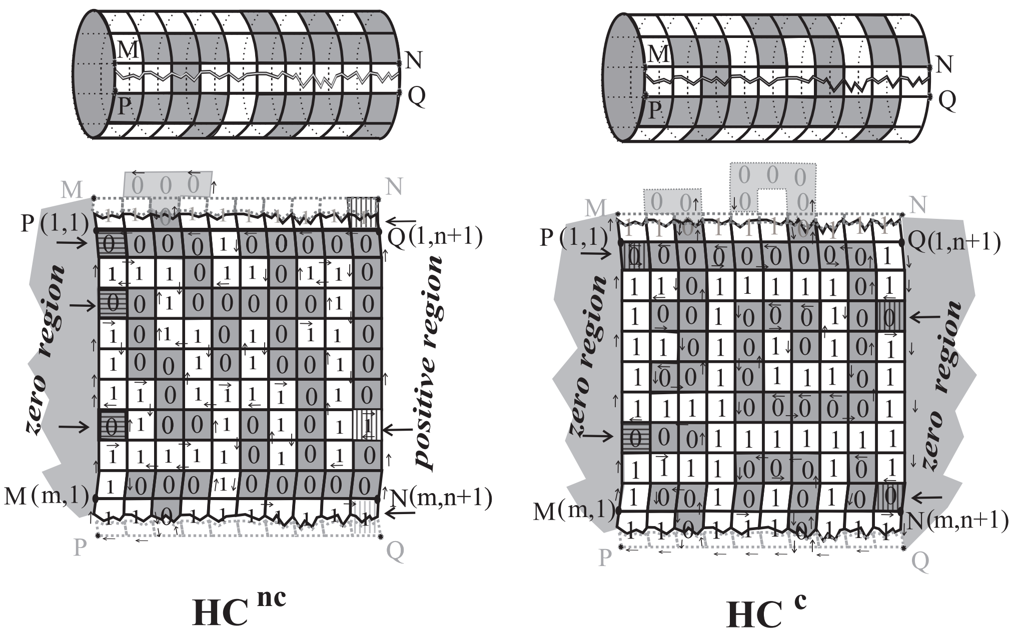

Fig. 3: Two types of Hamiltonian cycles.

$m(n+1)$ edges, we deduce that $m(n+1) \equiv m \pmod 2$. Thus, a HC^{nc} does not exist if both m and n are odd.

Similarly, if there exists a contractible Hamiltonian cycle, then $m(n+1)$ must be even, because there is an equal number of left and right steps, and an equal number of up and down steps. Hence, there is no HC^{c} if m is odd and n is even. □

Hamiltonicity of a graph has both a local (every vertex is visited exactly once) and a global (the subgraph is connected) aspect. For a HC^{nc}, the windows belonging to any one of the two regions induce a forest in the window lattice graph $W_{m,n}$. We call the trees in these forests ***zero trees*** (abbreviated ZTs) or ***positive trees*** (abbreviated PTs) depending on which region they belong to. Accordingly, their respective windows are called ***zero windows*** or ***positive windows***. Every zero tree contains exactly one window on the first column of $W_{m,n}$ from the set $\{w_{i,1} \mid 1 \le i \le m\}$ called the ***left root***, and every positive tree contains exactly one window on the last column of $W_{m,n}$ from the set $\{w_{i,n} \mid 1 \le i \le m\}$ called the ***right root***. For example, the HC^{nc} in Figure 3 has three zero trees with left roots $w_{1,1}, w_{3,1}$, and $w_{7,1}$ (striped), and two positive trees with right roots $w_{7,10}$, and $w_{10,10}$ (striped).

For a HC^{c}, the interior windows (they are marked with 1s in the HC^{c} in Figure 3) form a tree in $W_{m,n}$, but the exterior windows form a forest of ***exterior trees*** (abbreviated ETs). Note that only one ET from this forest contains exactly one window on the first column of $W_{m,n}$ (the ***left root***), and also exactly one window on the last column of $W_{m,n}$ (the ***right root***). We call this ET the ***split tree*** of the HC. Any ET different from the split tree contains either exactly one left root or exactly one right root, but not both. For example, the HC^{c} in Figure 3 has a split tree with the left root $w_{1,1}$ and the right root $w_{3,10}$, one ET with the left root $w_{7,1}$, and one ET with the right root $w_{9,10}$. For the purpose of this study, interior tree

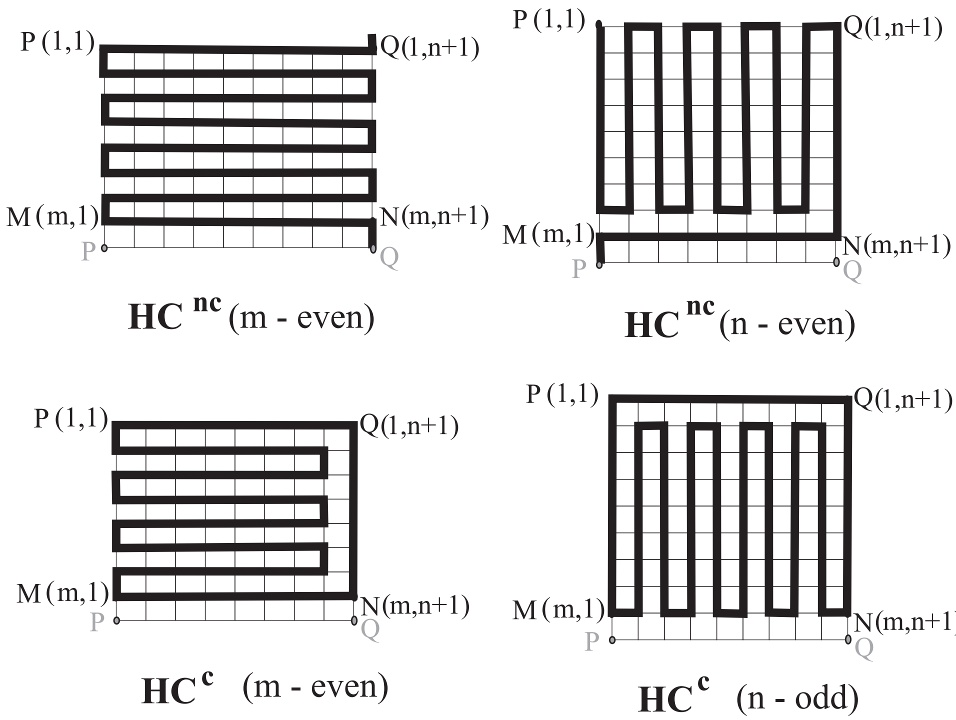

Fig. 4: The construction of the two types of Hamiltonian cycles.

and exterior trees are also called ***positive tree*** and ***zero trees***, and their windows are labeled by 1 and 0, respectively.

We need a few additional definitions to facilitate our discussion.

Definition 1 *Given a nonnegative integer word $d_1 d_2 \ldots d_m$, its* **support** *is defined as the binary word $\bar{d}_1 \bar{d}_2 \ldots \bar{d}_m$, where*

$$\bar{d}_i = \begin{cases} 1 & \text{if } d_i > 0, \\ 0 & \text{if } d_i = 0. \end{cases}$$

The **support** *of a nonnegative integer matrix $[d_{i,j}]$ is defined in a similar manner.*

Definition 2 *The factor u of a word v is called a b-***factor** *if it is a block of consecutive letters all of which equal to b. A b-factor of v is said to be* **maximal** *if it is not a proper factor of another b-factor of v.*

The approach described in the next section allows us to simultaneously analyze both types of Hamiltonian cycles.

3 First Characterization of HC

We associate with each Hamiltonian cycle of $C_m \times P_{n+1}$, for both types, a binary matrix $[a_{i,j}]_{m\times n}$, denoted A^{nc} for HC^{nc}, and A^c for HC^c, according to

$$a_{i,j} = \begin{cases} 1 & \text{if } w_{i,j} \text{ is a positive window,} \\ 0 & \text{otherwise.} \end{cases}$$

This matrix satisfies the following necessary conditions which are easy to verify (we adopt the convention that $a_{m+1,j} = a_{1,j}$, for $1 \le j \le n$).

Theorem 3.1 *The matrix $[a_{i,j}]_{m\times n}$ satisfies the following conditions:*

*[A1] (**First column condition**): The cyclic word $a_{1,1}a_{2,1}\dots a_{m,1} \in \{0,1\}^m$ has at least one 0 and does not contain the factor 00.*

*[A2] (**Adjacency condition**): For each i and j with $1 \le i \le m$ and $1 \le j \le n-1$,*

$$(a_{i,j}, a_{i+1,j}, a_{i,j+1}, a_{i+1,j+1}) \notin \{(1,1,1,1),(0,0,0,0),(0,1,1,0),(1,0,0,1)\}.$$

*[A3] (**Root condition**): Each connected component of the subgraph of $W_{m,n}$ induced by the 1-windows has a tree structure, and*

- *For HC^{nc}, every positive tree has exactly one square from the last column of $W_{m,n}$.*
- *For HC^{c}, there is exactly one positive tree.*

*[A4] (**Last column condition**): The cyclic word $a_{1,n}a_{2,n}\dots a_{m,n} \in \{0,1\}^m$ has*

- *For HC^{nc}, at least one 1, and does not contain the factor 11.*
- *For HC^{c}, at least one 0, and does not contain the factor 00.*

It is clear that every HC^{nc} (HC^{c}, resp.) yields exactly one matrix A^{nc} (A^{c} resp.) that satisfies conditions [A1]–[A4]. The converse is also true.

Theorem 3.2 *Every matrix $[a_{i,j}]_{m\times n}$ with entries from $\{0,1\}$ that satisfies conditions [A1]–[A4] determines a unique HC^{nc} (or HC^{c}) on $C_m \times P_{n+1}$.*

Proof: The entries in the matrix A can be used to label the windows of $C_m \times P_{n+1}$ with 0 and 1. Construct a subgraph on $C_m \times P_{n+1}$ by forming its edges as follows. Any edge neighboring a 0-window and a 1-window is selected. For A^{nc}, a left edge that joins the vertices $(m,1)$ and $(1,1)$, or the vertices $(i,1)$ and $(i+1,1)$, for $1 \le i \le m-1$, is selected if it is adjacent to a 1-window, and a right edge that joins $(m,n+1)$ to $(1,n+1)$ or $(i,n+1)$ to $(i+1,n+1)$, for $1 \le i \le m-1$, is selected if it is adjacent to a 0-window. For A^{c}, an edge on the left or right boundary is selected if it adjacent to a 1-window. For example, for the matrices in Figure 3, the edge between the vertices $(3,n+1)$ and $(4,n+1)$ is selected for A^{nc} but not for A^{c}.

The conditions [A1], [A2] and [A4] imply that this subgraph of $C_m \times P_{n+1}$ is a 2-factor. The global aspect of Hamiltonicity is provided by condition [A3]. The boundary of the positive region determines the uniqueness of the HC. □

We note that every possible first column in both A^{nc} and A^{c} and last column in A^{c} is a circular binary words of length m with no consecutive 0's, and is different from the word 1^m. Likewise, every possible last column in A^{nc} is a circular binary words of length m with no consecutive 1's, and is different from the word 0^m. It is well-known that the number of such binary words is $L_m - 1$, where L_m is the mth Lucas numbers with $L_0 = 2$, $L_1 = 1$, and $L_{k+1} = L_{k+1} + L_k$ for $k \ge 0$. See, for example, [1].

4 Second Characterization of HC

In this section, we propose an alternate characterization of the HCs on $C_m \times P_{n+1}$. Although it is more complicated, it leads to an effective way to compute the generating functions $\mathcal{H}_m^{nc}(x)$ and $\mathcal{H}_m^{c}(x)$. In the following discussion, A denotes either A^{nc} or A^c.

Definition 3 *Given a fixed positive integer k, two windows $w_{i,l}$ and $w_{j,s}$ that satisfy $a_{i,l} = a_{j,s} = 1$ (from either A^{nc} or A^c) and $l, s \leq k$ are said to be k-SIST (***surely in the same tree looking from the** k**-th column***) if and only if they belong to the same component in the subgraph of $W_{m,n}$ induced by $\{w_{p,t} \mid a_{p,t} = 1$ and $t \leq k\}$.*

For fixed k, being k-SIST is an equivalence relation on the set $\{w_{i,k} \mid a_{i,k} = 1$ and $1 \leq i \leq m\}$ and it has at most $\lfloor m/2 \rfloor$ equivalence classes. It is possible that two different classes eventually belong to the same positive tree of a Hamiltonian cycle on the entire cylindrical surface of $C_m \times P_{n+1}$. In other words, two windows that are not k-SIST could become ℓ-SIST for some integer $\ell > k$. However, we cannot tell whether it is true just from the first k columns of the matrix A.

Let $C^+ = \{2, 3, \ldots, \lfloor m/2 \rfloor + 1\}$. For any HC^{nc} or HC^c, we associate to the matrix A^{nc} or A^c from the first characterization a second matrix $[b_{i,j}]_{m \times n}$, denoted B^{nc} or B^c, where $b_{i,j} \in C^+ \cup \{0\}$, in the following way (see Figure 5). For each j:

(a) If $a_{i,j} = 0$, then $b_{i,j} = 0$.

(b) Partition the positive windows in the jth column into j-SIST equivalence classes, label all the windows within each equivalence class 2, 3, ..., according to the order in which the equivalence classes first appear within the jth column, from top to bottom.

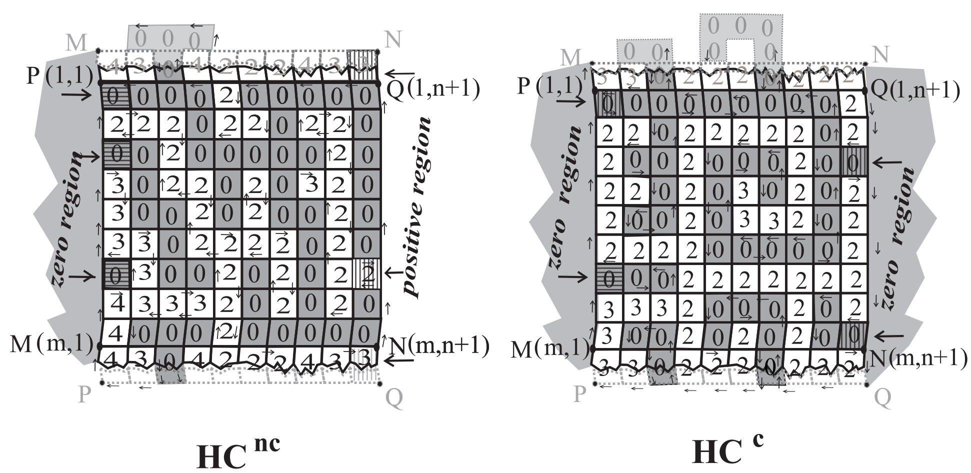

Fig. 5: The labeling of the windows of a HC^{nc} on $C_{10} \times P_{11}$, and a HC^c on $C_{10} \times P_{11}$.

Theorem 4.1 *The matrix $B = [b_{i,j}]_{m \times n}$ (either B^{nc} or B^c) satisfies the following properties (we adopt the convention $b_{m+1,j} = b_{1,j}$, and $b_{0,j} = b_{m,j}$, for $1 \leq j \leq n$):*

[B1] The first column $b_{1,1}b_{2,1}\ldots b_{m,1}$ is either

$$02^{d_1}03^{d_2}04^{d_3}\ldots 0(p+1)^{d_p}, \qquad p+\sum_{i=1}^{p} d_i = m,$$

or

$$2^{d_1}03^{d_2}04^{d_3}\ldots 0(p+1)^{d_p}02^{(m-p-d_1-d_2-\ldots-d_p)}, \qquad p+\sum_{i=1}^{p} d_i \le m,$$

where $p \ge 1$ is the number of 0s and $d_i > 0$ for $1 \le i \le p$.

[B2] The support of the matrix B, that is, the matrix $[a_{i,j}]_{m\times n}$, satisfies the adjacency condition [A2].

[B3] For $1 \le k \le n$, the kth column of the matrix B satisfies these conditions:

- *(a) If $b_{i,k} > 0$, where $1 \le i \le m$, then $b_{i-1,k}, b_{i+1,k} \in \{b_{i,k}, 0\}$.*
- *(b) If $b_{p_1,k}, b_{p_2,k}, \ldots, b_{p_l,k}$, where $l \le \lfloor m/2 \rfloor$, and $p_1 < p_2 < \cdots < p_l$, are the first appearance of the elements from C^+ in the kth column, then $b_{p_i,k} = i+1$.*
- *(c) If $k \ge 2$, $1 \le i, j \le m$, $i \ne j$, $b_{i,k-1} = b_{j,k-1}$, and $a_{i,k} = a_{j,k} = a_{i,k-1} = a_{j,k-1} = 1$, then $b_{i,k} = b_{j,k}$.*
- *(d) If $k \ge 2$, $1 \le i, j \le m$, $i \ne j$, $b_{i,k-1} = b_{j,k-1}$, $b_{i,k} = b_{j,k} = b$, and $a_{i,k-1} = a_{i,k} = 1$, then the kth column does not contain any b-factor that contains both $b_{i,k}$ and $b_{j,k}$.*
- *(e) If $k \ge 2$ and if v and u are two different maximal nonzero b-factors in the kth column, then there is exactly one sequence $v = v_1, v_2, \ldots, v_p = u$ of $p > 1$ different maximal b-factors in the kth column with the property that for every i with $1 \le i \le p-1$, in the $(k-1)$th column, there exists exactly one letter $b_{j_i,k-1}$ with $a_{j_i,k-1} = a_{j_i,k}$ for which $b_{j_i,k} \in v_i$, and there exists exactly one letter $b_{s_{i+1},k-1}$ with $a_{s_{i+1},k-1} = a_{s_{i+1},k}$ for which $b_{s_{i+1},k} \in v_{i+1}$ and $b_{j_i,k-1} = b_{s_{i+1},k-1}$; and $j_i \ne s_i$ for $1 < i < p$ (see Figure 6).*
- *(f) For $k \ge 2$ and for each number $b \in C^+$ that appears in the $(k-1)$th column, there must exist an integer i, where $1 \le i \le m$, for which $b_{i,k-1} = b$ and $b_{i,k} > 0$.*
- *(g) Every column has both positive and zero entries.*

[B4] The last column $b_{1,n}b_{2,n}\ldots b_{m,n}$ is

- *For HC^{nc},*

$$0^{d_1}20^{d_2}30^{d_3}\ldots p0^{d_p}(p+1)0^{m-p-d_1-d_2-\cdots-d_p}, \qquad p+\sum_{i=1}^{p} d_i = m,$$

or

$$20^{d_1}30^{d_2}40^{d_3}\ldots(p+1)0^{d_p}, \qquad p+\sum_{i=1}^{p} d_i \le m,$$

where $p \ge 1$ is the number of positive integers and $d_i > 0$ for $1 \le i \le p$.

- *For HC*^{c}*,*

$$2^{d_1}02^{d_2}02^{d_3}\dots02^{d_p}02^{m-p-d_1-d_2-\cdots-d_p}, \qquad p+\sum_{i=1}^{p} d_i = m,$$

or

$$02^{d_1}02^{d_2}02^{d_3}\dots02^{d_p}, \qquad p+\sum_{i=1}^{p} d_i \le m,$$

where $p \ge 1$ *is the number of 0s and* $d_i > 0$ *for* $1 \le i \le p$*.*

Proof: First, a few remarks.

- [B1] and [B2] follow from the definition of the matrix B.
- [B3a]: Two windows belonging to the same equivalence class must be associated with the same number.
- [B3b]: This follows from the definition of the matrix B.
- [B3c]: If $w_{i,k-1}$ and $w_{j,k-1}$ are $(k-1)$-SIST, and if the windows $w_{i,k}$, $w_{j,k}$, $w_{i,k-1}$ and $w_{j,k-1}$ are from the positive region, then the windows $w_{i,k}$ and $w_{j,k}$ must be k-SIST.
- [B3d]: If the opposite is true, we would obtain a cycle in a positive tree, which is impossible.
- [B3e]: If we can conclude by knowing the first k columns that v and u are in the same tree, then there is exactly one path from v to u in their positive tree via some windows from the previous column, that is, the $(k-1)$th column.
- [B3f]: Every positive tree must "reach" the last column.
- [B3g]: For a HC^{nc}, the unique path in $W_{m,n}$ starting in a positive window from the first column and finishing in the last column must cross every column. For a HC^c, the unique split tree must cross every column as well. Furthermore, the occurrence of a column with no zero window would imply that the corresponding subgraph in $C_m \times P_{n+1}$ is not connected, which is impossible.
- [B4]: This follows from the definition of the matrix B.

Based on these remarks, it is not difficult to verify the properties listed in the theorem. □

Theorem 4.2 *Every integer matrix* $B = [b_{i,j}]_{m\times n}$ *with entries from* $C^+ \cup \{0\}$ *satisfying properties [B1]–[B4] determines a unique HC on* $C_m \times P_{n+1}$*.*

Proof: It suffices to show that the support of B (which could be either B^{nc} or B^c) satisfies conditions [A1]–[A4] in Theorem 3.1. It is clear that properties [B1], [B2] and [B4] imply conditions [A1], [A2] and [A4], respectively. Properties [B3d] and [B3e] yield the forest structure for the subgraph of $W_{m,n}$ induced by positive windows (since no cycle can occur). The properties [B3c], [B3f] and [B4] for B^{nc} assert that every positive tree in $W_{m,n}$ has exactly one right root. For B^c, the property [B3f] implies that for every positive window there exists a path starting from this window and finishing in the last column of $W_{m,n}$, and the property [B4] guarantees that the subgraph of $W_{m,n}$ induced by the positive windows is connected. □

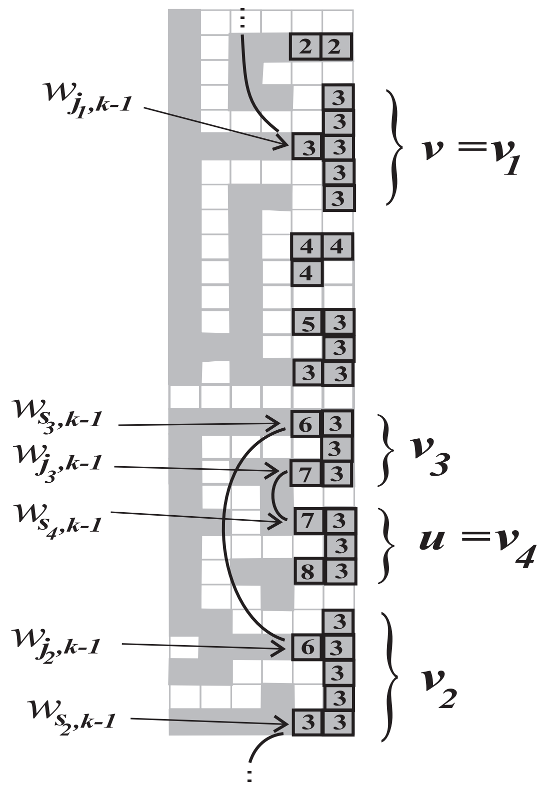

Fig. 6: The property [B3e].

5 Technique for Enumerating Hamiltonian Cycles

For each integer $m \geq 2$, we construct a digraph $\mathcal{D}_m$ in the following manner. The set of vertices $V(\mathcal{D}_m)$ consists of all possible columns in the matrix B. Hence, $V(\mathcal{D}_m)$ consists of integer words $d_1d_2\ldots d_m$ from the alphabet $C^+ \cup \{0\}$. A directed line joins the vertex v to the vertex u, where $v, u \in V(\mathcal{D}_m)$, if and only if the vertex v (as an integer word $b_{1,k-1}b_{2,k-1}\ldots b_{m,k-1}$) might be the previous column for the vertex u (as a word $b_{1,k}b_{2,k}\ldots b_{m,k}$). Consequently, these two words satisfy conditions [B2] and [B3]. The subset of $V(\mathcal{D}_m)$ that consists of all possible first columns in the matrix B (condition [B1]) is represented by $\mathcal{F}_m$. The subset of $V(\mathcal{D}_m)$ consisting of all possible last columns in the matrix B (condition [B4]) is denoted $\mathcal{L}_m^{nc}$ or $\mathcal{L}_m^{c}$ depending on whether the HC is non-contractible or contractible.

The problem of enumerating HC^{nc} or HC^{c} on $C_m \times P_{n+1}$ now becomes the problem of enumerating oriented walks of the length $n-1$ in the digraph $\mathcal{D}_m$ with the initial vertices in the set $\mathcal{F}_m$, and the final vertices in set $\mathcal{L}_m^{nc}$ or $\mathcal{L}_m^{c}$. We note that Faase [7] used a similar method to enumerate spanning subgraphs of $G \times P_n$ that meet certain conditions.

Because of the rotational symmetry and reflection symmetry of $C_m \times P_n$, we can further simplify the digraph $\mathcal{D}_m$ by identifying some of its vertices, hence reducing its adjacency (transfer) matrix T_m to a smaller size. By doing so, we obtain the multidigraph $\mathcal{D}_m^*$ instead of $\mathcal{D}_m$ with transfer matrix T_m^*.

The computation of the generating functions

$$\mathcal{H}_m^{nc}(x) = \sum_{n\geq 0}^{\infty} h_m^{nc}(n+1)x^n \qquad \text{and} \qquad \mathcal{H}_m^{c}(x) = \sum_{n\geq 0}^{\infty} h_m^{c}(n+1)x^n$$

is rather routine (see Theorem 4.7.2 in [18]). It is obvious that

$$\mathcal{H}_m(x) = \sum_{n\geq 0}^{\infty} h_m(n+1)x^n = \mathcal{H}_m^{nc}(x) + \mathcal{H}_m^{c}(x). \tag{1}$$

These generating functions are rational functions. Their denominators are determined by the characteristic polynomials of the adjacency matrices. Table 1 displays, for $3 \leq m \leq 10$, the numbers of vertices in $\mathcal{F}_m$, $\mathcal{D}_m$ and $\mathcal{D}_m^*$, as well as the degrees of the denominators in these generating functions, which determine the orders of the recurrence relations for h_m^{nc} and h_m^c.

We find an interesting upper bound of $|V(\mathcal{D}_m|$. A column in the matrix $[b_{i,j}]_{m\times n}$ can be viewed as a word. Let its maximal nonzero b-factors, in the order of their appearance, be p_1-factor, p_2-factor, ... , p_k-factor. Call $p_1p_2\dots p_k$ a ***positive truncated word***. For example, the positive truncated words correspond to the 2nd and 6th columns of B^c in Figure 5 are 22233 and 2322, respectively. Every truncated word v has two properties:

- If a letter $s \geq 3$ appears in v, then, in accordance with the property [B3b], each number from $\{2,\dots,s-1\}$ must have appeared at least once before it. In other words, if we remove the duplicated letters, the remaining letters will form the word 234... .
- If $abab$ is a subsequence of the word v, then $a = b$ (because of the properties [B3e] and [B1]).

A word over the alphabet $\{2,\dots,k+1\}$ that possesses the above-mentioned properties is called a ***color word***. The number of color words of length k is the Catalan number $C_k = \frac{1}{k+1}\binom{2k}{k}$, see [3, 16]. Using a relation between Catalan and Motzkin numbers described in [6], we obtain the following corollary.

Corollary 5.1 *An upper bound on the number of vertices of digraph $\mathcal{D}_m$ is*

$$|V(\mathcal{D}_m)| \leq 2\sum_{k=1}^{\lfloor m/2\rfloor}\binom{m}{2k}C_k = 2(M_m - 1),$$

where C_m is the mth Catalan number and M_m is mth Motzkin number.

In light of Corollay 5.1, we would like to remark that we could use Motzkin words to encode the columns. See, for example, [19].

6 Computational Results

Based on the discussion in the previous section, we use Pascal programs to compute the adjacency matrices of the multidigraphs $\mathcal{D}_m^*$, from which we obtain $\mathcal{H}_m^{nc}(x)$ and $\mathcal{H}_m^c(x)$. The results are summarized in Table 1. Notice that the numbers $|V(\mathcal{D}_m)|$ and $2(M_m - 1)$ are equal when m is odd.

m	3	4	5	6	7	8	9	10
$\lvert\mathcal{F}_m\rvert = L_m - 1$	3	6	10	17	28	46	75	122
$2(M_m - 1)$	6	16	40	100	252	644	1668	4374
$\lvert V(\mathcal{D}_m)\rvert$	6	12	40	64	252	364	1668	2234
$\lvert V(\mathcal{D}^*_m)\rvert$	2	4	8	14	30	44	128	172
deg den. $\mathcal{H}_m(x)$	1	2	3	7	12	20	51	74
deg den. $\mathcal{K}_m(x)$	1	2	3	6	12	20	51	67
deg den. $\mathcal{H}^{nc}_m(x)$, $\mathcal{H}^{c}_m(x)$	2	4	6	13	24	40	102	141

Tab. 1: The computational results from Pascal programs.

Since $\mathcal{H}^{nc}_m(x)$ and $\mathcal{H}^{c}_m(x)$ are derived from the same transfer matrix, their denominators are identical. After adding the two rational functions to form $\mathcal{H}_m(x)$, the new denominator may have a lesser degree. In fact, numerical data reveal that the degree is reduced by roughly one-half, see Table 1.

Upon further examination of the factorization of the denominator, we conclude that a better way to study them is to introduce the function

$$\mathcal{K}_m(x) = \mathcal{H}^{c}_m(x) - \mathcal{H}^{nc}_m(x), \tag{2}$$

such that, together with (1),

$$\mathcal{H}^{nc}_m(x) = \frac{1}{2}\left(\mathcal{H}_m(x) - \mathcal{K}_m(x)\right), \tag{3}$$

$$\mathcal{H}^{c}_m(x) = \frac{1}{2}\left(\mathcal{H}_m(x) + \mathcal{K}_m(x)\right). \tag{4}$$

Since both $\mathcal{H}_m(x)$ and $\mathcal{K}_m(x)$ are rational functions, we can express them as

$$\mathcal{H}_m(x) = \overline{\mathcal{H}}_m(x) + \frac{p_m(x)}{q_m(x)} \qquad \text{and} \qquad \mathcal{K}_m(x) = \overline{\mathcal{K}}_m(x) + \frac{r_m(x)}{s_m(x)},$$

for some polynomials $\overline{\mathcal{H}}_m(x)$, $\overline{\mathcal{K}}_m(x)$, $p_m(x)$, $q_m(x)$, $r_m(x)$ and $s_m(x)$, such that $\deg(p_m) < \deg(q_m)$ and $\deg(r_m) < \deg(s_m)$.

The denominator $q_m(x)$ of the generating function $\mathcal{H}_m(x)$ provides important information about the numbers $h_m(n)$. Let its degree be d_m. Then $\chi_m(t) = t^{d_m} q_m(1/t)$ is the characteristic polynomial which determines the recurrence relation that $h_m(n)$ satisfies. It has d_m nonzero roots (the characteristic roots) over $\mathbb{C}$, name them $\lambda_{m,i}$ so that $|\lambda_{m,1}| \geq |\lambda_{m,2}| \geq \cdots \geq |\lambda_{m,d_m}|$. We can write

$$q_m(x) = \prod_{i=1}^{d_m}(1 - \lambda_{m,i}x).$$

Note that the zeros of $q_m(x)$ are $\lambda^{-1}_{m,i}$. For the sake of brevity, we shall still call $\lambda_{m,i}$s the ***characteristic roots*** of $q_m(x)$. It is a routine exercise to show that, if $\lambda_{m,i}$s are simple (hence distinct) roots, then

$$\frac{p_m(x)}{q_m(x)} = \sum_{i=1}^{d_m} \frac{\alpha_i}{1 - \lambda_{m,i}x},$$

so that for sufficiently large n

$$h_m(n+1) = \sum_{i=1}^{d_m} \alpha_i \lambda_{m,i}^n,$$

where $\alpha_i = -\lambda_{m,i} p_m(\lambda_{m,i}^{-1})/q_m'(\lambda_{m,i}^{-1})$. The solution is more complicated if some of the $\lambda_{m,i}$s are repeated roots. Nonetheless, if $\lambda_{m,1}$ is a simple positive root such that $\lambda_{m,1} > |\lambda_{m,2}|$, then

$$h_m(n+1) \sim \alpha_1 \lambda_{m,1}^n,$$

in which the formula for α_1 given above still holds. See the following sections for illustrations of our discussion.

6.1 The Thin Grid Cylinder $C_2 \times P_{n+1}$

We find $h_2^{nc}(n) = 2$ and $h_2^c(n) = 2$, hence $h_2(n) = 4$, for all $n \geq 1$.

6.2 The Thin Grid Cylinder $C_3 \times P_{n+1}$

Let $V(\mathcal{D}_3) = \{v_1, v_2, \ldots, v_6\}$. We obtain the following:

$$\begin{array}{l} v_1 = (2,2,0) \\ v_2 = (2,0,2) \\ v_3 = (0,2,2) \\ v_4 = (0,0,2) \\ v_5 = (0,2,0) \\ v_6 = (2,0,0) \end{array} \qquad T_3 = \begin{bmatrix} 0 & 0 & 0 & 0 & 1 & 1 \\ 0 & 0 & 0 & 1 & 0 & 1 \\ 0 & 0 & 0 & 1 & 1 & 0 \\ 0 & 1 & 1 & 0 & 0 & 0 \\ 1 & 0 & 1 & 0 & 0 & 0 \\ 1 & 1 & 0 & 0 & 0 & 0 \end{bmatrix} \qquad \begin{array}{l} \mathcal{F}_3 = \{v_1, v_2, v_3\} \\ \mathcal{L}_3^{nc} = \{v_4, v_5, v_6\} \\ \mathcal{L}_3^c = \{v_1, v_2, v_3\} \\ \\ T_3^* = \begin{bmatrix} 0 & 2 \\ 2 & 0 \end{bmatrix} \end{array}$$

$$\begin{array}{ll} h_3^{nc}(2k-1) = 0, \quad k \geq 1 & h_3^c(2k) = 0, \quad k \geq 1 \\ h_3^{nc}(2) = 6 & h_3^c(1) = 3 \\ h_3^{nc}(4) = 24 & h_3^c(3) = 12 \\ h_3^{nc}(6) = 96 & h_3^c(5) = 48 \\ h_3^{nc}(8) = 384 & h_3^c(7) = 192 \end{array}$$

The characteristic polynomial of T_3^* is $x^2 - 4$. Because of Cayley-Hamilton theorem, we obtain the recurrence relations $h_3^{nc}(n) = 4h_3^{nc}(n-2)$ and $h_3^c(n) = 4h_3^c(n-2)$. The generating functions are

$$\mathcal{H}_3^{nc}(x) = \frac{6x}{1-4x^2} = \frac{3}{2(1-2x)} - \frac{3}{2(1+2x)},$$
$$\mathcal{H}_3^c(x) = \frac{3}{1-4x^2} = \frac{3}{2(1-2x)} + \frac{3}{2(1+2x)}.$$

Therefore,

$$\mathcal{H}_3(x) = \frac{3}{1-2x} \qquad \text{and} \qquad \mathcal{K}_3(x) = \frac{3}{1+2x}.$$

The denominator of $\mathcal{H}_3(x)$ yields the recurrenece relation

$$h_3(n) = 2h_3(n-1), \qquad n \geq 2.$$

Since $\frac{3}{1-2x} = 3\sum_{k=0}^{\infty} 2^k x^k$, we obtain the following simple formula for $h_3(n)$.

Theorem 6.1 *For $n \geq 1$, the number of Hamiltonian cycles in $C_3 \times P_{n+1}$ is*

$$h_3(n) = 3 \cdot 2^{n-1}.$$

6.3 *The Thin Grid Cylinder* $C_4 \times P_{n+1}$

Let $V(\mathcal{D}_4) = \{v_1, v_2, \ldots, v_{12}\}$. We obtain the following:

$$\begin{array}{l} v_1 = (2,2,2,0) \\ v_2 = (2,2,0,2) \\ v_3 = (2,0,2,2) \\ v_4 = (2,0,3,0) \\ v_5 = (0,2,2,2) \\ v_6 = (0,2,0,3) \\ v_7 = (0,0,0,2) \\ v_8 = (0,0,2,0) \\ v_9 = (0,2,0,0) \\ v_{10} = (2,0,0,0) \\ v_{11} = (2,0,2,0) \\ v_{12} = (0,2,0,2) \end{array} \qquad T_4 = \begin{bmatrix} 0&0&0&0&0&0&0&1&1&1&1&0 \\ 0&0&0&0&0&0&1&0&1&1&0&1 \\ 0&0&0&0&0&0&1&1&0&1&1&0 \\ 1&0&1&1&0&0&0&0&0&0&0&0 \\ 0&0&0&0&0&0&1&1&1&0&0&1 \\ 0&1&0&0&1&1&0&0&0&0&0&0 \\ 0&1&1&0&1&1&0&0&0&0&0&0 \\ 1&0&1&1&1&0&0&0&0&0&0&0 \\ 1&1&0&0&1&1&0&0&0&0&0&0 \\ 1&1&1&1&0&0&0&0&0&0&0&0 \\ 0&0&0&0&0&0&0&1&0&1&1&0 \\ 0&0&0&0&0&0&1&0&1&0&0&1 \end{bmatrix}$$

$$\begin{array}{l} \mathcal{F}_4 = \{v_1, v_2, \ldots, v_6\} \\ \mathcal{L}_4^{nc} = \{v_4, v_6, v_7, v_8, v_9, v_{10}\} \\ \mathcal{L}_4^{c} = \{v_1, v_2, v_3, v_5, v_{11}, v_{12}\} \end{array}$$

$$T_4^* = \begin{bmatrix} 0&0&3&1 \\ 2&1&0&0 \\ 3&1&0&0 \\ 0&0&2&1 \end{bmatrix}$$

$$\begin{array}{ll} h_4^{nc}(1) = 2 & h_4^{c}(1) = 4 \\ h_4^{nc}(2) = 14 & h_4^{c}(2) = 8 \\ h_4^{nc}(3) = 34 & h_4^{c}(3) = 48 \\ h_4^{nc}(4) = 170 & h_4^{c}(4) = 136 \\ h_4^{nc}(5) = 530 & h_4^{c}(5) = 612 \\ h_4^{nc}(6) = 2230 & h_4^{c}(6) = 2032 \\ h_4^{nc}(7) = 7714 & h_4^{c}(7) = 8192 \\ h_4^{nc}(8) = 30258 & h_4^{c}(8) = 29104 \\ h_4^{nc}(9) = 109378 & h_4^{c}(9) = 112164 \\ h_4^{nc}(10) = 416766 & h_4^{c}(10) = 410040 \\ h_4^{nc}(11) = 1534722 & h_4^{c}(11) = 1550960 \\ h_4^{nc}(12) = 5777562 & h_4^{c}(12) = 5738360 \\ h_4^{nc}(13) = 21441682 & h_4^{c}(13) = 21536324 \end{array}$$

The generating functions are:

$$\mathcal{H}_4^{nc}(x) = \frac{2(1+5x-5x^2+x^3)}{(1-4x+x^2)(1+2x-x^2)} = \frac{3-x}{1-4x+x^2} - \frac{1-x}{1+2x-x^2},$$
$$\mathcal{H}_4^{c}(x) = \frac{4}{(1-4x+x^2)(1+2x-x^2)} = \frac{3-x}{1-4x+x^2} + \frac{1-x}{1+2x-x^2},$$

from which we obtain

$$\mathcal{H}_4(x) = \frac{2(3-x)}{1-4x+x^2} \qquad \text{and} \qquad \mathcal{K}_4(x) = \frac{2(1-x)}{1+2x-x^2},$$

and the recurrence relation

$$h_4(n) = 4h_4(n-1) - h_4(n-2), \qquad n \geq 3.$$

After decomposing into partial fractions, we find

$$\frac{2(3-x)}{1-4x+x^2} = \frac{9+5\sqrt{3}}{3} \cdot \frac{1}{1-\big(2+\sqrt{3}\,\big)x} + \frac{9-5\sqrt{3}}{3} \cdot \frac{1}{1-\big(2-\sqrt{3}\,\big)x}.$$

This leads to the next result.

Theorem 6.2 *For $n \geq 1$, the number of Hamiltonian cycles in $C_4 \times P_{n+1}$ is*

$$h_4(n) = \frac{1}{3}\Big[\big(9+5\sqrt{3}\,\big)\big(2+\sqrt{3}\,\big)^{n-1} + \big(9-5\sqrt{3}\,\big)\big(2-\sqrt{3}\,\big)^{n-1}\Big],$$

and $h_4(n) \sim \frac{1}{3}\big(9+5\sqrt{3}\,\big)\big(2+\sqrt{3}\,\big)^{n-1}$.

6.4 The Thin Grid Cylinder $C_5 \times P_{n+1}$

We find $|V(\mathcal{D}_5)| = 40$, $V(\mathcal{D}_5^*) = \{v_1, \ldots, v_8\}$, and

$$\begin{aligned} v_1 &= (2,2,2,2,0) \\ v_2 &= (2,2,0,3,0) \\ v_3 &= (0,0,0,0,2) \\ v_4 &= (0,0,2,0,3) \\ v_5 &= (2,0,2,0,0) \\ v_6 &= (2,0,0,2,2) \\ v_7 &= (2,0,2,2,0) \\ v_8 &= (2,0,0,0,2) \end{aligned} \qquad T_5^* = \begin{bmatrix} 0 & 0 & 4 & 0 & 3 & 0 & 0 & 0 \\ 0 & 0 & 0 & 2 & 0 & 2 & 0 & 0 \\ 4 & 3 & 0 & 0 & 0 & 0 & 0 & 0 \\ 3 & 2 & 0 & 0 & 0 & 0 & 0 & 0 \\ 0 & 0 & 0 & 0 & 0 & 0 & 2 & 2 \\ 0 & 0 & 0 & 0 & 0 & 0 & 2 & 2 \\ 0 & 0 & 3 & 0 & 2 & 0 & 0 & 0 \\ 0 & 0 & 0 & 2 & 0 & 2 & 0 & 0 \end{bmatrix}$$

$$\begin{array}{ll} h_5^{nc}(2k-1) = 0, \quad k \geq 1 & h_5^{c}(2k) = 0, \quad k \geq 1 \\ h_5^{nc}(2) = 30 & h_5^{c}(1) = 5 \\ h_5^{nc}(4) = 850 & h_5^{c}(3) = 160 \\ h_5^{nc}(6) = 24040 & h_5^{c}(5) = 4520 \\ h_5^{nc}(8) = 680040 & h_5^{c}(7) = 127860 \\ h_5^{nc}(10) = 19236840 & h_5^{c}(9) = 3616880 \end{array}$$

We obtain

$$\mathcal{H}_5^{nc}(x) = \frac{10x(x^2+3)}{1-28x^2-8x^4-4x^6} = \frac{5}{1-6x+4x^2-2x^3} - \frac{5}{1+6x+4x^2+2x^3},$$

$$\mathcal{H}_5^{c}(x) = \frac{5(4x^2+1)}{1-28x^2-8x^4-4x^6} = \frac{5}{1-6x+4x^2-2x^3} + \frac{5}{1+6x+4x^2+2x^3}.$$

Hence,

$$\mathcal{H}_5(x) = \frac{10}{1-6x+4x^2-2x^3} \qquad \text{and} \qquad \mathcal{K}_5(x) = \frac{10}{1+6x+4x^2+2x^3}.$$

Due to its complexity, we will not display the explicit formula for $h_5(n)$. Numerically, $\lambda_{5,1} \approx 5.31863$, and $\lambda_{5,2}, \lambda_{5,3} \approx 0.34069 \pm 0.50987i$.

6.5 The Thin Grid Cylinder $C_6 \times P_{n+1}$

$$\begin{aligned}
\mathcal{H}_6^{nc}(x) &= 2 + 62x + 278x^2 + 4178x^3 + 27710x^4 + 314354x^5 + 2468810x^6 + 24770708x^7 \\
&\quad + 210413420x^8 + 1998760352x^9 + 17601771968x^{10} + 163119159176x^{11} \\
&\quad + 1460403914672x^{12} + 13382718140000x^{13} + 120722781112208x^{14} \\
&\quad + 1100628776882000x^{15} + 9962793339446672x^{16} \\
&\quad + 90619491133658576x^{17} + 821568683907144752x^{18} \\
&\quad + 7464893093725073072x^{19} + 67726216376743239056x^{20} + \cdots, \\
\mathcal{H}_6^{c}(x) &= 6 + 24x + 498x^2 + 2832x^3 + 35964x^4 + 263736x^5 + 2779014x^6 + 22869384x^7 \\
&\quad + 222067212x^8 + 1927331160x^9 + 18039580560x^{10} + 160435712688x^{11} \\
&\quad + 1476851478768x^{12} + 13281906604320x^{13} + 121340682078768x^{14} \\
&\quad + 1096841495972016x^{15} + 9986006600900208x^{16} + 90477210822238320x^{17} \\
&\quad + 822440758133272176x^{18} + 7459547916670820976x^{19} \\
&\quad + 67758978401907276048x^{20} + \cdots, \\
\mathcal{H}_6(x) &= \frac{2(4 + 7x + x^2 - 27x^3 - 26x^4 - 20x^5 - 3x^6)}{1 - 9x - 10x^3 + 28x^4 + 36x^5 + 32x^6 + 12x^7}, \\
\mathcal{K}_6(x) &= \frac{2(2 - 11x + 14x^2 - 11x^3 - x^4 + x^5)}{1 + 4x - 10x^2 + 16x^3 - 16x^4 + 4x^5 + 4x^6}.
\end{aligned}$$

The denominator $q_6(x)$ has seven simple roots, three real and four complex, and $\lambda_{6,1} \approx 9.07807$.

6.6 The Thin Grid Cylinder $C_7 \times P_{n+1}$

We find $\mathcal{H}_7(x) = p_7(x)/q_7(x)$, and $\mathcal{K}_7(x) = r_7(x)/s_7(x)$, where

$$\begin{aligned}
\mathcal{H}_7^{nc}(x) &= 126x + 18452x^3 + 2861964x^5 + 444486280x^7 + 69048910000x^9 \\
&\quad + 10726732430288x^{11} + 1666401898058352x^{13} + 258876295158900832x^{15} \\
&\quad + 40216553455854426560x^{17} + 6247660438430706481984x^{19} + \cdots, \\
\mathcal{H}_7^{c}(x) &= 7 + 1484x^2 + 229698x^4 + 35663964x^6 + 5539931796x^8 + 860620499760x^{10} \\
&\quad + 133697577587000x^{12} + 20769976722986288x^{14} + 3226625529605854320x^{16} \\
&\quad + 501257787787122948736x^{18} + 77870632467402116097056x^{20} + \cdots, \\
p_7(x) &= 7(1 + 6x - 22x^2 - 120x^3 - 178x^4 + 72x^5 + 580x^6 + 616x^7 + 264x^8 + 72x^9 + 16x^{10}), \\
q_7(x) &= 1 - 12x - 18x^2 + 112x^3 + 440x^4 + 772x^5 + 196x^6 \\
&\quad - 2064x^7 - 3724x^8 - 2040x^9 - 496x^{10} - 128x^{11} + 16x^{12},
\end{aligned}$$

and $r_7(x) = p_7(-x)$, and $s_7(x) = q_7(-x)$.

6.7 The Thin Grid Cylinder $C_8 \times P_{n+1}$

Again, we have $\overline{\mathcal{H}}_8(x) = \overline{\mathcal{K}}_8(x) = 0$,

$$\begin{aligned}
\mathcal{H}_8^{nc}(x) &= 2 + 254x + 1794x^2 + 82138x^3 + 1012930x^4 + 30717374x^5 + 481369234x^6 \\
&+ 12070287370x^7 + 214585144402x^8 + 4886085696654x^9 \\
&+ 92880601782338x^{10} + 2011688161424970x^{11} + 39622707294281746x^{12} \\
&+ 836009740378418718x^{13} + 16778455639135020178x^{14} + \cdots, \\
\mathcal{H}_8^{c}(x) &= 8 + 64x + 4320x^2 + 44288x^3 + 1575288x^4 + 22337664x^5 + 605992784x^6 \\
&+ 10215798448x^7 + 242178636928x^8 + 4475508186384x^9 \\
&+ 98989761676840x^{10} + 1920787160180224x^{11} + 40975264449253872x^{12} \\
&+ 815884428197037360x^{13} + 17077909293201385648x^{14} + \cdots, \\
p_8(x) &= 2(5 + 44x - 430x^2 + 33x^3 + 93x^4 + 1471x^5 + 4596x^6 + 6807x^7 \\
&+ 8263x^8 + 2751x^9 - 2482x^{10} - 5126x^{11} - 4711x^{12} - 2094x^{13} \\
&- 1406x^{14} + 450x^{15} + 580x^{16} - 132x^{17} + 32x^{18} + 40x^{19}), \\
q_8(x) &= 1 - 23x + 34x^2 + 345x^3 + 218x^4 - 22x^5 - 2919x^6 - 5041x^7 \\
&- 8806x^8 - 11998x^9 - 5873x^{10} + 1318x^{11} + 4467x^{12} + 11373x^{13} \\
&+ 3848x^{14} - 584x^{15} + 1018x^{16} - 928x^{17} + 84x^{18} + 72x^{19} - 40x^{20}, \\
r_8(x) &= 2(3 - 80x + 476x^2 - 1143x^3 + 303x^4 + 4917x^5 - 8670x^6 - 2291x^7 \\
&+ 19477x^8 - 13315x^9 - 16780x^{10} + 19224x^{11} + 6103x^{12} - 9974x^{13} \\
&- 1352x^{14} + 3926x^{15} - 1796x^{16} + 644x^{17} - 168x^{18} + 16x^{19}), \\
s_8(x) &= 1 + 5x - 104x^2 + 529x^3 - 1548x^4 + 1830x^5 + 3915x^6 - 13527x^7 \\
&+ 7182x^8 + 20914x^9 - 31027x^{10} - 9214x^{11} + 35037x^{12} + 1205x^{13} \\
&- 19590x^{14} + 890x^{15} + 5770x^{16} - 2048x^{17} + 588x^{18} - 184x^{19} + 16x^{20}.
\end{aligned}$$

6.8 The Thin Grid Cylinder $C_9 \times P_{n+1}$

$$\begin{aligned}
\mathcal{H}_9^{nc}(x) &= 510x + 351258x^3 + 276018090x^5 + 218915964618x^7 + 173923080282474x^9 \\
&+ 138226113213225360x^{11} + 109864493967924549384x^{13} \\
&+ 87323767337933601800838x^{15} + 69407973132514050824027916x^{17} \\
&+ 55167927811346067821770238916x^{19} \\
&+ 43849442381504976630009404305836x^{21} + \cdots, \\
\mathcal{H}_9^{c}(x) &= 9 + 12348x^2 + 9806292x^4 + 7769376972x^6 + 6169925169414x^8 \\
&+ 4903042542453720x^{10} + 3896923927019062734x^{12} \\
&+ 3097380080814655131414x^{14} + 2461902328199084994926838x^{16} \\
&+ 1956807009306757665486727506x^{18} \\
&+ 1555340096869096304430909957438x^{20} + \cdots.
\end{aligned}$$

We find $\overline{\mathcal{H}}_9(x) = \overline{\mathcal{K}}_9(x) = 0$. Like the cases of $m = 3, 5, 7$, we also have $r_9(x) = p_9(-x)$ and $s_9(x) = q_9(-x)$. However, since $\deg(p_9) + 1 = \deg(q_9) = 51$, we will not attempt to list these polynomials in their entirety.

6.9 The Thin Grid Cylinder $C_{10} \times P_{n+1}$

$$\begin{aligned}
\mathcal{H}_{10}^{nc}(x) &= 2 + 1022x + 10652x^2 + 1505612x^3 + 32718482x^4 + 2701992092x^5 + 79977736982x^6 \\
&\quad + 5099841986502x^7 + 179765502917052x^8 + 9933064485778002x^9 \\
&\quad + 387981888303174142x^{10} + 19745599426500473672x^{11} \\
&\quad + 819563054782862759352x^{12} + 39759941758256449144532x^{13} \\
&\quad + 1710706207634346787583712x^{14} + 80696804239003472593910602x^{15} + \cdots \\
\mathcal{H}_{10}^{c}(x) &= 10 + 160x + 34850x^2 + 621720x^3 + 62999960x^4 + 1641664580x^5 + 116791523380x^6 \\
&\quad + 3817933082020x^7 + 224360971248960x^8 + 8381173203185000x^9 \\
&\quad + 441980748032029010x^{10} + 17866610320162579120x^{11} \\
&\quad + 884945074721799980580x^{12} + 37484874131377414126080x^{13} \\
&\quad + 1789870555278304706976120x^{14} + 77942162101044243981212480x^{15} + \cdots .
\end{aligned}$$

We close by mentioning that $\overline{\mathcal{H}}_{10}(x) = \overline{\mathcal{K}}_{10}(x) = 0$, $\deg(p_{10}) + 1 = \deg(q_{10}) = 74$, and $\deg(r_{10}) + 1 = \deg(s_{10}) = 67$.

7 Asymptotic Values

Let ρ_m be the radius of convergence for $\mathcal{H}_m(x)$. The coefficients of $\mathcal{H}_m(x)$ are non-negative, Pringsheim's Theorem (see, for example, [8]) states that it has a singularity at $x = \rho_m$. Since we assume that $q_m(x) = \prod_{i=1}^{d_m}(1 - \lambda_{m,i}x)$, where $|\lambda_{m,1}| \geq |\lambda_{m,2}| \geq \cdots \geq |\lambda_{m,d_m}| \neq 0$, one of the characteristic roots with the largest moduli must be real, positive, and equal to $1/\rho_m$. We may assume it is $\lambda_{m,1}$. For brevity, we denote it θ_m. If $\theta_m = \lambda_{m,1} > |\lambda_{m,2}|$, then θ_m is the dominant root, and

$$h_m(n+1) \sim a_m \theta_m^n,$$

where $a_m = -\theta_m p_m(\theta_m^{-1})/q_m'(\theta_m^{-1})$. Do we always have $|\lambda_{m,1}| > |\lambda_{m,2}|$? The fact that the transfer matrix T_m^* is nonnegative points to the Perron-Frobenius theorem for an answer.

Let M be a nonnegative square matrix. We say that M is irreducible if, for every i and j, there exists a positive integer $k = k(i,j)$ such that $(M^k)_{ij} > 0$. This is equivalent to saying that the multidigraph G_M with adjacency matrix M is strongly connected. The matrix M is said to be primitive if $A^\gamma > 0$ for some positive integer γ. For example, the matrix

$$T_3^* = \begin{bmatrix} 0 & 2 \\ 2 & 0 \end{bmatrix}$$

is irreducible but not primitive, and T_4^* is primitive because $T_4^{*2} > 0$. The period or order of cyclicity of M, labeled by g, can be defined as the greatest common divisor of the lengths of the directed cycles in G_M [12]. From the Perron-Frobenius theory (see, for example, [12]), g is the number of eigenvalues of

M having the largest modulus. In particular, a primitive matrix is an irreducible nonnegative matrix with $g = 1$, it has exactly one dominant characteristic root. We find that, for $3 \le m \le 10$, the transfer matrix T^*_m is irreducible, but it is primitive only when m is even. Accordingly, we shall study the cases of odd and even m separately.

When m is odd, Theorem 2.1 implies that

$$h_m(n) = \begin{cases} h^{nc}_m(n) & \text{if } n \text{ is even,} \\ h^c_m(n) & \text{if } n \text{ is odd.} \end{cases} \tag{5}$$

Hence $\mathcal{H}^{nc}_m(x)$ comes from the odd terms of $\mathcal{H}_m(x)$, and $\mathcal{H}^c_m(x)$ from the even terms. This means

$$\begin{aligned} \mathcal{H}^{nc}_m(x) &= \frac{1}{2}\left(\mathcal{H}_m(x) - \mathcal{H}_m(-x)\right), \\ \mathcal{H}^{c}_m(x) &= \frac{1}{2}\left(\mathcal{H}_m(x) + \mathcal{H}_m(-x)\right). \end{aligned}$$

Hence, $\mathcal{K}_m(x) = \mathcal{H}_m(-x)$ when m is odd. Since $\mathcal{H}^{nc}_m(x)$ and $\mathcal{H}^c_m(x)$ share the same denominator $q_m(x)q_m(-x)$, both sequences h^{nc}_m and h^c_m satisfy a linear recurrence relation of order $2d_m$. However, $q_m(x)q_m(-x)$ is an even function, so it is a polynomial of degree d_m in x^2. Thus, the subsequences of nonzero terms $\{h^{nc}_m(2n)\}_{n\ge1}$ and $\{h^c_m(2n-1)\}_{n\ge1}$ satisfy a linear recurrence relation of order d_m. Because of (5), it is clear that, for the nonzero terms, the asymptotic behavior of $h^{nc}_m(n)$ and $h^c_m(n)$ is same as that of $h_m(n)$. More precisely, $h^{nc}_m(2n) \sim h_m(2n)$, and $h^c_m(2n+1) \sim h_m(2n+1)$.

If the transfer matrix $\mathcal{D}^*_m$ is irreducible, then it would have g_m dominant characteristic roots, where g_m denotes the period of $\mathcal{D}^*_m$. The fact that $q_m(x)q_m(-x)$, the denominator that $\mathcal{H}^{nc}_m(x)$ and $\mathcal{H}^c_m(x)$ share, is a polynomial in x^2 suggests that $\mathcal{D}^*_m$ is a bipartite graph. If this can be confirmed, then g_m must be even. In fact, it contains the following directed cycle of length 2: $u_1u_2u_1$, where u_1 and u_2 are vertices (written as words) in $\mathcal{D}^*_m$

$$u_1 = 222\cdots20, \qquad u_2 = 000\cdots02.$$

See Figure 4 and note that, because of the rotational symmetry, the vertex $22\cdots202$ is identified to $22\cdots220$, as well $20\cdots00$ to $00\cdots02$. We conclude that $g_m = 2$, so the two dominant characteristic roots of $\mathcal{D}^*_m$ must be $\pm\theta_m$. This in turn implies that θ_m is the sole dominant characteristic root of $q_m(x)$. Consequently, we deduce that, for odd m,

$$h^{nc}_m(2n) \sim a_m\theta_m^{2n-1} \qquad \text{and} \qquad h^c_m(2n+1) \sim a_m\theta_m^{2n},$$

provided that T^*_m is irreducible, and $\mathcal{D}^*_m$ is a bipartite graph. Our computational data reveal that $\mathcal{D}^*_3$, $\mathcal{D}^*_5$, $\mathcal{D}^*_7$, $\mathcal{D}^*_9$ are bipartite multidigraphs.

For even m, we note that $\mathcal{D}^*_m$ contains loops. For example, there is a loop around the vertex representing the word $2030\cdots((m+2)/2)0$, see Figure 4. We conclude that, if T^*m is irreducible (recall that our computational data confirm that the matrix T^*_m is indeed irreducible for $m \le 10$), then $g_m = 1$. But the dominant characteristic root can come from either $\mathcal{H}_m(x)$ or $\mathcal{K}_m(x)$. Our computational data reveal that, for $m \le 10$, the radius of convergence for $\mathcal{K}_m(x)$ is greater than that of $\mathcal{H}_m(x)$. This, together with (3) and (4), imply that the dominant characteristic root of both $\mathcal{H}^{nc}(x)$ and $\mathcal{H}^c_m(x)$ comes from $\mathcal{H}_m(x)$. Hence,

$$h^{nc}_m(n+1) \sim \frac{a_m}{2}\,\theta^n_m \qquad \text{and} \qquad h^c_m(n+1) \sim \frac{a_m}{2}\,\theta^n_m.$$

This immediately proves that $h^{nc}_m(n) \sim h^c_m(n)$ when $m = 2, 4, 6, 8, 10$. Is it always true when m is even?

8 Concluding Remarks and Open Problems

Our computational data affirm that for $3 \leq m \leq 10$, the denominator $q_m(x)$ has only one real positive dominant characteristic root θ_m, see Table 2. Our main conjecture is:

m	θ_m	a_m
3	2	3
4	3.73205080756887729352744634151	5.8867513459481288225457439025
5	5.31862821775018565910968015332	5.6485507137110988135657454508
6	9.07807499686426137037316693063	9.3759765980423268475201653010
7	12.46396683154921167484924057847	9.5114780466647699643291510197
8	20.49548062885849319891140410573	14.6698889618659187804647562240
9	28.19283279845402927227773603077	15.4543604331204162432381530254
10	45.31795107579019470088202555080	22.7172562899371282508816262267

Tab. 2: The approximate values of θ_m and a_m.

Conjecture 1 *For each even $m \geq 4$,*

$$h_m^{nc}(n+1) \sim h_m^c(n+1) \sim \frac{a_m}{2}\, \theta_m^n,$$

where $a_m = -\theta_m p_m(\theta_m^{-1})/q_m'(\theta_m^{-1})$.

As we have discussed in the previous section, the validity this conjecture, and other related asymptotic relations, can be completely resolved if we can settle the following open problems:

1. Is T_m^* irreducible for all $m \geq 3$? Note that this has been confirned for $m \leq 10$.
2. Is $\mathcal{D}_m^*$ bipartite when m is odd? Again, this has been confirmed up to $m = 9$.
3. Does the dominant characteristic root remain in $\mathcal{H}_m$ when m is even? This is equivalent to showing that the radius of convergence for $\mathcal{K}_m(x)$ is greater than that of $\mathcal{H}_m(x)$.

Our computational data suggest further problems for investigation:

4. Is the sequence generated by $\mathcal{K}_m(x)$ always alternating? In other words, do we always have $h_m^c(2k) < h_m^{nc}(2k)$ and $h_m^c(2k+1) > h_m^{nc}(2k+1)$?

We close our discussion with three more interesting questions:

6. What is an appropriate combinatorial interpretation for $\mathcal{K}_m(x)$?
7. Can we define a labeling of the windows such that a single transfer matrix can be used to obtain the generating function $\mathcal{H}_m(x)$ directly? If such a transfer matrix does exist, its characteristic polynomial should be $\chi_m(t)$ mentioned in Section 6. (Recall that the matrices obtained in [2] for graph $C_m \times P_n$ are transfer matrices for sequences $h_m(n)$, but obtained by a labeling of the vertices of $C_m \times P_n$. We additionally verified that they are indeed primitive for $m \leq 12$.)
8. Can we find some similar properties of sequences $h_m(n)$, $h_m^{nc}(n)$ and $h_m^c(n)$ for the case of thick cylinder $P_m \times C_n$ (m is kept constant, whereas n grows)?

Acknowledgments

We are indebted to the anonymous referees. Their generous and valuable suggestions helped us reshape the exposition in Sections 6–8. We are grateful to Dragoš Cvetković and Jasmina Tekić for their constructive comments and suggestions for improving the paper. The authors thank Bojana Pantić for many valuable comments and help in the implementation of the Pascal programs.

References

[1] A.T. Benjamin, and J.J. Quinn, Recounting Fibonacci and Lucas identities, *College Math. J.*, **30** (1999), 359–366.

[2] O. Bodroža-Pantić, B. Pantić, I. Pantić, and M. Bodroža-Solarov, Enumeration of Hamiltonian cycles in some grid graphs, *MATCH Commun. Math. Comput. Chem.*, **70:1** (2013), 181–204.

[3] O. Bodroža-Pantić, H. Kwong, and M. Pantić, Some new characterizations of Hamiltonian cycles in triangular grid graphs, submitted for publication.

[4] O. Bodroža-Pantić, and R. Tošić, On the number of 2-factors in rectangular lattice graphs, *Publications De L'Institut Mathématique*, **56** (70) (1994), 23–33.

[5] D.M. Cvetković, M. Doob, and H. Sachs, *Spectra of Graphs — Theory and Application*, VEB Deutscher Verlag der Wissenschaften, Berlin, 1982.

[6] R. Donaghey, and L.W. Shapiro, Motzkin numbers, *J. Combin. Theory, Series A*, **23** (1997), 291–301.

[7] F.J. Faase, The number of specific spanning subgraphs of the graphs $G \times P_n$, *Ars Combin.* **49** (1998), 129–154.

[8] P. Flajolet, and R. Sedgewick, *Analytic Combinatorics*, Cambridge University Press, 2009.

[9] M.J. Golin, Y.C. Leung, Y. Wang, and X. Yong, Counting structures in grid-graphs, cylinders and tori using transfer matrices: survey a new results (extended abstract), *The Proceedings of SIAM ALENEX/ANALCO Workshop — Analytic Algorithmics and Combinatorics (ANALCO05)*, Canada, 2005.

[10] J.L. Jacobsen, Exact enumeration of Hamiltonian circuits, walks and chains in two and three dimensions, *J. Phys. A: Math. Theor.*, **40** (2007), 14667–14678.

[11] А.М. Караваев, Кодирование состояний в методе матрицы переноса для подсчета гамильтоновых циклов на прямоугольных решетках, цилиндрах и торах, Информационные процессы, **11** (2011), no. 4, 476–499.

[12] B.P. Kitchens, *Symbolic Dynamics- One-sided, Two-sided and Countable State Markov Shifts*, Springer, 1997.

[13] G. Kreweras, Dénombrement des Cycles Hamiltoniens dans un Rectangle Quadrillé, *Europ. J. Combin.*, **13** (1992), 473–467.

[14] Y.H.H. Kwong, Enumeration of Hamiltonian cycles in $P_4 \times P_n$ and $P_5 \times P_n$, *Ars Combin.*, **33** (1992), 87–96.

[15] Y.H.H. Kwong, and D.G. Rogers, A matrix method for counting hamiltonian cycles on grid graphs, *Europ. J. Combin.*, **15** (1994), 277–283.

[16] J. Quaintance, and H. Kwong, A combinatorial interpretation of the Catalan and Bell number difference tables, *Integers*, **13** (2013), #A29.

[17] T.G. Schmalz, G.E. Hite, and D.J. Klein, Compact self-avoiding circuits on two dimensional lattice, *J. Phys. A: Math. Theor.*, **17** (1984), 445–453.

[18] R.P. Stanley, *Enumerative Combinatorics, Vol. I*, Cambridge University Press, Cambridge, 2002.

[19] R. Stoyan, and V. Strehl, Enumeration of hamiltonian circuits in rectangular grids, *J. Combin. Math. Combin. Comput.*, **21** (1996), 109–127.

[20] R. Tošić, O. Bodroža, Y.H.H. Kwong, and H.J. Straight, On the number of Hamiltonian cycles of $P_4 \times P_n$, *Indian J. Pure Appl. Math.*, **21** (1990), 403–409.